

Direct evidence for sequential dissociation of gas-phase Fe(CO)₅ via a singlet pathway upon excitation at 266 nm

Ph. Wernet^{1*}, T. Leitner^{1#}, I. Josefsson², T. Mazza³, P.S. Miedema¹⁺, H. Schröder^{1,5}, M. Beye¹⁺,
K. Kunnus^{1,5§}, S. Schreck^{1,5&}, P. Radcliffe³, S. Düsterer⁴, M. Meyer³, M. Odelius^{2*}, A.
Föhlisch^{1,5}

¹ Institute for Methods and Instrumentation for Synchrotron Radiation Research, Helmholtz-Zentrum Berlin für Materialien und Energie GmbH, Albert-Einstein-Strasse 15, 12489 Berlin, Germany

² Department of Physics, Stockholm University, AlbaNova University Center, 106 91 Stockholm, Sweden

³ European XFEL GmbH, Holzkoppel 4, 22869 Schenefeld, Germany

⁴ Deutsches Elektronen-Synchrotron DESY, Notkestrasse 85, 22607 Hamburg, Germany

⁵ Institut für Physik und Astronomie, Universität Potsdam Karl-Liebnecht-Strasse 24/25, 14476 Potsdam, Germany

* Corresponding authors: Philippe Wernet (wernet@helmholtz-berlin.de), Michael Odelius (odelius@fysik.su.se)

Present address: Uppsala-Berlin joint Laboratory for next generation photoelectron spectroscopy, Albert-Einstein-Strasse 15, 12489 Berlin, Germany, and Dept. of Physics and Astronomy, Uppsala University, Box 516, 751 20 Uppsala, Sweden

+ Present address: DESY, FS-FLASH, Notkestrasse 85, 22607 Hamburg, Germany

§ Present address: PULSE Institute, SLAC National Accelerator Laboratory, Menlo Park, CA 94025, USA

& Present address: Department of Physics, Stockholm University, AlbaNova University Center, 106 91 Stockholm, Sweden

Abstract

We prove the hitherto hypothesized sequential dissociation of $\text{Fe}(\text{CO})_5$ in the gas phase upon photoexcitation at 266 nm via a singlet pathway with time-resolved valence and core-level photoelectron spectroscopy at an x-ray free-electron laser. Valence photoelectron spectra are used to identify free CO molecules and to determine the time constants of step-wise dissociation to $\text{Fe}(\text{CO})_4$ within the temporal resolution of the experiment and further to $\text{Fe}(\text{CO})_3$ within 3 ps. Fe 3p core-level photoelectron spectra directly reflect the singlet spin state of the Fe center in $\text{Fe}(\text{CO})_5$, $\text{Fe}(\text{CO})_4$, and $\text{Fe}(\text{CO})_3$ showing that the dissociation exclusively occurs along a singlet pathway without triplet-state contribution. Our results are important for assessing intra- and intermolecular relaxation processes in the photodissociation dynamics of the prototypical $\text{Fe}(\text{CO})_5$ complex in the gas phase and in solution and they establish time-resolved core-level photoelectron spectroscopy as a powerful tool for determining the multiplicity of transition metals in photochemical reactions of coordination complexes.

The photochemistry of metal carbonyls has been the subject of numerous investigations^{1, 2} and $\text{Fe}(\text{CO})_5$ has always occupied a prominent role as a prototypical benchmark case for organometallic photoreactions³. To date, the photo-induced dissociation of metal carbonyls^{4, 5}, specifically $\text{Fe}(\text{CO})_5$ ⁶⁻¹⁰, has attracted great interest. In the quest for understanding what determines reactivity in organometallic photoreactions, it appears essential to understand how intra- and inter-molecular relaxation processes interplay as both determine photochemical reactivity^{1-3, 11}. Contrasting photodissociation of $\text{Fe}(\text{CO})_5$ in the gas phase and in solution thus helps understanding how fundamental processes of bond dissociation and formation, intersystem crossing and vibrational relaxation influence the excited-state dynamics of the reactive intermediates on fs to ps time scales^{12, 13}. Owing to its reduced complexity and the missing solute-solvent interactions, gas-phase $\text{Fe}(\text{CO})_5$ can be regarded as a reference case and the question occurs about how well we actually know this reference.

As summarized by Poliakoff and Turner in 2001¹⁴, the loss of multiple CO molecules upon UV photolysis of gas-phase $\text{Fe}(\text{CO})_5$ (singlet ground state) has been established early on^{6, 15, 16} while the time scale of photodissociation remained unknown as well as whether dissociation proceeded sequentially or synchronously. Similarly, the multiplicity of the transient intermediates $\text{Fe}(\text{CO})_4$ and $\text{Fe}(\text{CO})_3$ remained elusive. The ground states of $\text{Fe}(\text{CO})_4$ and $\text{Fe}(\text{CO})_3$ in rare-gas matrices were found to be triplets^{16, 17}. The triplet ground state of gas-phase $\text{Fe}(\text{CO})_4$ was confirmed theoretically¹⁸⁻²⁰ hence suggesting a triplet pathway from excited singlet-state $\text{Fe}(\text{CO})_5$ to triplet-state $\text{Fe}(\text{CO})_4$ via intersystem crossing¹⁹. In a seminal investigation of gas-phase photodissociation of $\text{Fe}(\text{CO})_5$ upon excitation at 266 nm with femtosecond-resolution optical ionization experiments²¹, Fuss and co-workers accurately measured time constants ranging from tens of fs to few ps albeit without the ability to uniquely assign species. They further assumed that intersystem crossing could not occur on such short time scales and thus proposed a sequential singlet pathway. Dissociation was proposed to proceed from excited singlet-state $\text{Fe}(\text{CO})_5$ to excited singlet-state $\text{Fe}(\text{CO})_4$ ($^1\text{A}_1$) within less than 100 fs with subsequent dissociation of a second CO to $\text{Fe}(\text{CO})_3$ with a time constant of 3.3 ps²¹. Singlet-state $\text{Fe}(\text{CO})_4$ in the gas phase was indeed detected with time-resolved electron diffraction by Ihee, Zewail and co-workers²² but their temporal resolution was limited to 10-20 ps and excitation was indirect with two-photon absorption at 620 nm.

An experimental proof for sequential $\text{Fe}(\text{CO})_5$ photodissociation in the gas phase is hence still missing. This is essential as successive dissociation motivates designing strategies to stabilize the reactive intermediate $\text{Fe}(\text{CO})_4$ for subsequent reactions. Furthermore, experimental verification of singlet-state $\text{Fe}(\text{CO})_4$ at short time scales of 1 ps or less and thus validation or disproval of the proposed singlet²¹ or triplet pathway¹⁹ is still missing. This is important because the triplet ground state of $\text{Fe}(\text{CO})_4$ was detected in solution^{7, 8} thus indicating a corresponding reaction barrier²⁰. The incomplete knowledge of gas-phase $\text{Fe}(\text{CO})_5$ photodissociation is largely due to limitations of currently established experimental techniques. These limitations are overcome in the present study with optical pump and x-ray probe spectroscopy at the x-ray free-electron laser FLASH²³ and the open questions are answered. The new insight is based on probing the reaction intermediates with time-resolved valence and core-level photoelectron spectroscopy²⁴⁻³¹.

$\text{Fe}(\text{CO})_5$ was pumped at 266 nm and probed with soft x-ray pulses from the x-ray free-electron laser FLASH in Hamburg (Germany)²³ with time-resolved x-ray photoelectron spectroscopy (repetition rate 10 Hz, x-ray photon energy 123 eV, photon-energy bandwidth 0.1 eV, x-ray pulse energies of 20-40 $\mu\text{J}/\text{pulse}$ before the monochromator, spot size 280 μm horizontal, 400 μm vertical, Gaussian FWHM, x-ray pulse duration 100 fs). A comparison of rare-gas photoelectron spectra measured at these conditions with previously published and with previously measured rare-gas spectra with the same set up at FLASH showed no indication for an influence of the comparably low probe-pulse energy on our measurements. $\text{Fe}(\text{CO})_5$ and CO were prepared as effusive jets in an ultrahigh-vacuum chamber where photodecomposition of $\text{Fe}(\text{CO})_5$ prior to measurements was prevented by keeping it in the dark and using fresh sample for each measurement shift. Photoelectron kinetic energies were analyzed with a magnetic-bottle-type time-of-flight electron spectrometer (electron-energy bandwidth 0.4-1.2 eV for valence photoelectron kinetic energies 118-103 eV and 1.5 eV for Fe 3p core-level photoelectron kinetic energies 60 eV). Pump and probe pulses propagated nearly collinearly through the interaction region. Pump pulses at 266 nm were obtained by third-harmonic generation of a Ti:Sa laser (pulse duration 150 fs, pulse energy 25 $\mu\text{J}/\text{pulse}$, pump fluence 7 mJ/cm^2 , pump peak intensity $1.2 \cdot 10^{11} \text{ W}/\text{cm}^2$, spot size 500 μm horizontal, 700 μm vertical, Gaussian FWHM). The pump-probe signals were found to saturate at higher pump fluences and no indication of multiphoton or other non-linear effects by the pump laser were detected. Our pump intensity is higher than the $10^9 \text{ W}/\text{cm}^2$

used in ²¹ but much lower than the 10^{14} W/cm² used in ⁶ or the 10^{13} W/cm² for 2-photon excitation with 620 nm in ²². In a post processing analysis, data were sorted to correct for unintentional changes of pump-probe delay times (detected with a streak camera correlating radiation of the optical laser and dipole radiation from FLASH). This average (in contrast to shot-to-shot) correction ensured correction of long-term drifts (minutes/hours) of the pump-probe delay. A shot-to-shot correction, as required for better temporal resolution, could unfortunately not be realized at the time of data acquisition at FLASH for the present study. More details of the experimental design and realization will be presented in a forthcoming publication.

The kinetic rate-model fit was performed with the following set of equations:

$$\text{Fe(CO)}_5 \quad N_5(t) = 1 - f_s(w, t)$$

$$\text{Fe(CO)}_4 \quad N_4(t) = f_d(\tau_4, w, t)$$

$$\text{Fe(CO)}_3 \quad N_3(t) = 1 - N_5(t) - N_4(t) = f_s(w, t) - f_d(\tau_4, w, t)$$

$$\text{CO1} \quad N_{\text{CO1}}(t) = 1 - N_5(t) = f_s(w, t)$$

$$\text{CO2} \quad N_{\text{CO2}}(t) = N_3(t) = f_s(w, t) - f_d(\tau_4, w, t)$$

$$\text{With} \quad f_s(w, t) = \frac{1}{2} \left[1 + \text{erf} \left(\frac{2\sqrt{\ln 2}}{w} t \right) \right]$$

$$\text{And} \quad f_d(\tau_4, w, t) = e^{-(t-\beta)/\tau_4} f_s(w, t - 2\beta) \quad \text{with} \quad \beta = \frac{w^2}{\tau_4(16 \ln 2)}$$

$N_i(t)$ are the fitted populations of the respective species, $f_s(w, t)$ is the convolved step function for a temporal resolution w (Gaussian FWHM), $f_d(\tau_4, w, t)$ is the convolved exponential decay for a temporal resolution w and the lifetime (time constant) τ_4 for the decay, and $N_5(t)$ encodes the depletion of Fe(CO)_5 . The parameter w (temporal resolution) was fitted to 1 ± 0.3 ps (Gaussian FWHM). The time constant τ_4 for exponential decay of Fe(CO)_4 and rise of CO2 was fitted to 2.8 ± 1.9 ps.

Valence-electron binding energies were computed in multiconfigurational self-consistent-field (MCSCF) calculations similar to the approach of Grell et al.³² as energy differences between the CASPT2(10,10) initial ground and final ionic states with one electron less and they included scalar relativistic effects and spin-orbit coupling³³. The geometries of the complexes were optimized at the CASPT2(12,12) level. Within the crystal-field multiplet model (CFM)^{34, 35} Fe 3p photoelectron spectra of singlet ground-state (1A_1) and the excited triplet-state (3B_2) of Fe $3d^8 4s^0$ were calculated. Minimal assumptions were introduced to robustly extract the spectral contrast between low-spin (singlet) and high-spin (triplet) states by matching the valence energy-level structure of $Fe(CO)_5$, $Fe(CO)_4$ and $Fe(CO)_3$ from the CFM calculation with that of the MCSCF calculations by using parameters $10Dq=1$ eV and $Ds=-5$ eV in the CFM calculations. For each final ionic state a Lorentzian profile with a FWHM of 1.2 eV was calculated reflecting lifetime broadening of the core-hole states³⁶ and all Lorentzians were summed and convoluted with the experimental bandwidth of 1.5 eV (Gaussian FWHM reflecting combined photon-energy and electron-kinetic-energy bandwidths).

Our time-resolved valence photoelectron spectra are shown in Figure 1. The spectrum of $Fe(CO)_5$ (Fig. 1 (a)) was studied earlier and shows peaks assigned to Fe 3d and CO σ and π orbitals^{37, 38}. The difference spectra extracted for the indicated time delays (Fig. 1 (b)) exhibit the rise of new species (peaks 1 and 2) and depletion of $Fe(CO)_5$ (mainly at 9.5 and 15 eV). We concentrate here on peaks 1 and 2 and note that all other changes in the spectrum can be consistently interpreted.

Since our temporal resolution is 1 ps we do not expect to probe the initial dynamics of excited-state $Fe(CO)_5$ on the 100 fs time scale and rather focus on the dissociation dynamics with the formation of $Fe(CO)_4$ and $Fe(CO)_3$. With the CO valence photoelectron spectrum (Fig. 1(a)) measured under identical conditions shortly after the pump-probe measurements of $Fe(CO)_5$, peak 1 in the transient spectra in Fig. 1(b) can be unambiguously assigned to free CO molecules arising from dissociation. Its intensity continues rising up to the maximum measured delay of 6 ps while $Fe(CO)_5$ depletion saturates at a delay of 0.7 ps. This already indicates successive dissociation where $Fe(CO)_5$ depletes during a first dissociation step only and CO continues rising as it is formed in one or more consecutive dissociation steps.

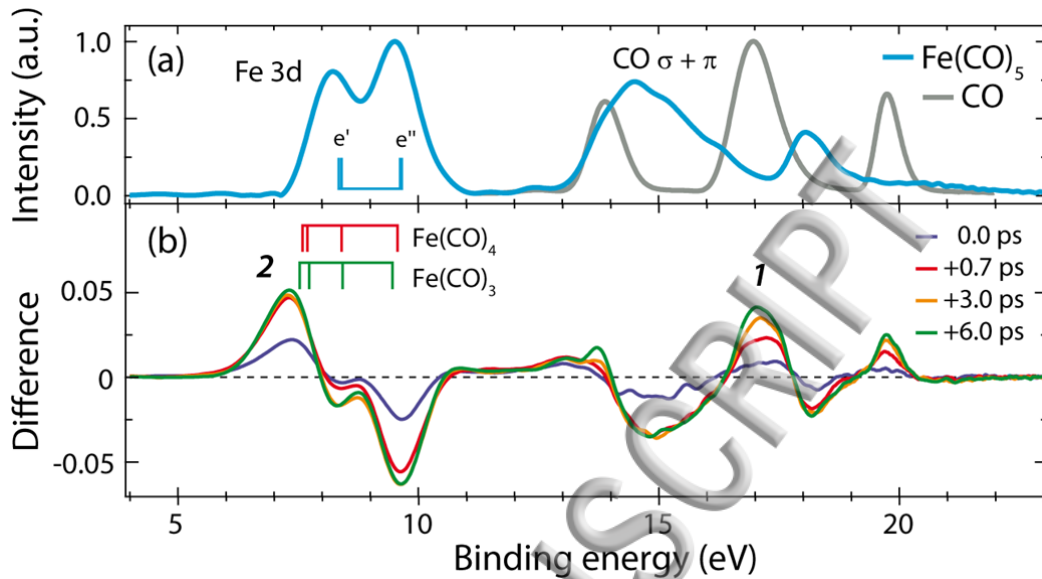


Figure 1. (a) Valence photoelectron spectra of $\text{Fe}(\text{CO})_5$ and CO (photon energy 123 eV, intensities normalized to one at maximum). (b) Difference spectra at indicated delay times after excitation of $\text{Fe}(\text{CO})_5$ at 266 nm (positive delays correspond to pump before probe pulses, the spectrum of unpumped molecules at -3 ps was subtracted from the measured intensities at the given delays). Calculated final ionic-state energies are indicated by vertical bars for $\text{Fe}(\text{CO})_5$ in (a) and $\text{Fe}(\text{CO})_4$ and $\text{Fe}(\text{CO})_3$ in (b) with ionization from, with increasing binding energy, (e' , e'') orbitals in $\text{Fe}(\text{CO})_5$, (a_1 , b_2 , b_1 , a_2) in $\text{Fe}(\text{CO})_4$ and (a' , a'' , a' and a'') in $\text{Fe}(\text{CO})_3$.

The temporal evolution of intensities of peaks 1 and 2 is plotted in Fig. 2 and compared to a kinetic rate-model fit employing the minimum necessary number of parameters to fit the experimental data.

The steadily increasing intensity of peak 1 is found to result from two components. First, it increases within temporal resolution due to the appearance of a first free CO from $\text{Fe}(\text{CO})_5$ to $\text{Fe}(\text{CO})_4$ dissociation (CO1 in Fig. 2(a)). Second, it rises due to a second free CO from successive $\text{Fe}(\text{CO})_4$ to $\text{Fe}(\text{CO})_3$ dissociation (CO2 in Fig. 2(a), exponential rise with a time constant of 2.8 ± 1.9 ps). Our data thus directly validate successive $\text{Fe}(\text{CO})_5$ photodissociation at 266 nm as proposed by Fuss and co-workers²¹ in two consecutive steps. Extending their work, our valence photoelectron spectroscopy results allow for unambiguously assigning species to the measured time constants.

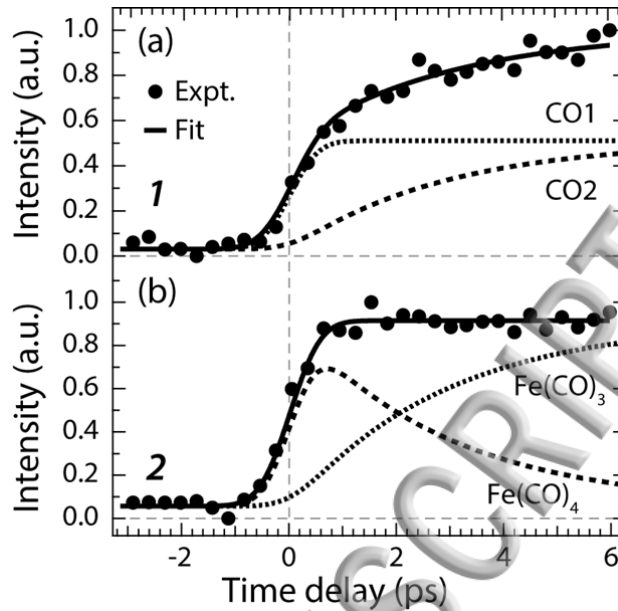


Figure 2. Integrated intensities of CO, Fe(CO)₄ and Fe(CO)₃ valence photoelectron peaks (1 and 2 in Fig. 1) versus pump-probe delay time (closed circles, integration intervals 16.6-17.3 eV for 1 and 6.6-8 eV for 2, intensities normalized to one at maximum). The best fit of a kinetic model is shown as solid lines with the respective components.

With our multiconfigurational self-consistent-field (MCSCF) calculations using a basis set of triple-zeta valence with polarization quality (ANO-RCC-VTZP) shown as bar diagrams in Fig. 1(b), peak 2 in particular can be assigned to Fe(CO)₄ and Fe(CO)₃. Consistent with our findings on CO evolution in Fig. 2(a), peak 2 is found to rise within the temporal resolution and to stay constant thereafter (Fig. 2(b)). Its intensity evolution apparently results from the mutually varying populations of Fe(CO)₄ and Fe(CO)₃. The intensity component of Fe(CO)₄ rises within 1 ps due to Fe(CO)₅ to Fe(CO)₄ dissociation paralleling CO1 evolution and it decays exponentially with a fitted time constant of 2.8 ± 1.9 ps concomitant with the rise of CO2 due to successive dissociation of Fe(CO)₄ to Fe(CO)₃ (the Fe(CO)₃ signal rises concomitantly).

Having established the kinetics, we now turn to exploiting the element- and site-specificity of core-level photoelectron spectroscopy. The measured time-resolved Fe 3p photoelectron spectra, their differences for selected delays and the temporal evolution of selected spectral regions with the kinetic rate-model fit are shown in Fig. 3.

The peak at 63 eV in Fig. 3(a) is due to emission from the Fe 3p core level in $\text{Fe}(\text{CO})_5$ ³⁸ thereby establishing elemental specificity of our probe. It depletes with increasing time delay due to $\text{Fe}(\text{CO})_5$ dissociation at the expense of the increasing peak 1 at 60-61 eV assigned to the photofragments (Fig. 3(b)). The temporal evolution of peak 1 is well explained with our kinetic model (Fig. 3(c)) with the mutually varying contributions of $\text{Fe}(\text{CO})_4$ and $\text{Fe}(\text{CO})_3$. This is consistent with a chemical shift of the Fe 3p photoelectron peak by minus 2-3 eV when going from $\text{Fe}(\text{CO})_5$ to $\text{Fe}(\text{CO})_4$ or $\text{Fe}(\text{CO})_3$. The details of this chemical shift and a closer inspection of the time-dependent changes in the valence photoelectron spectra will be analyzed in a forthcoming publication together with a discussion about how to, potentially, further distinguish spectroscopically between $\text{Fe}(\text{CO})_4$ and $\text{Fe}(\text{CO})_3$.

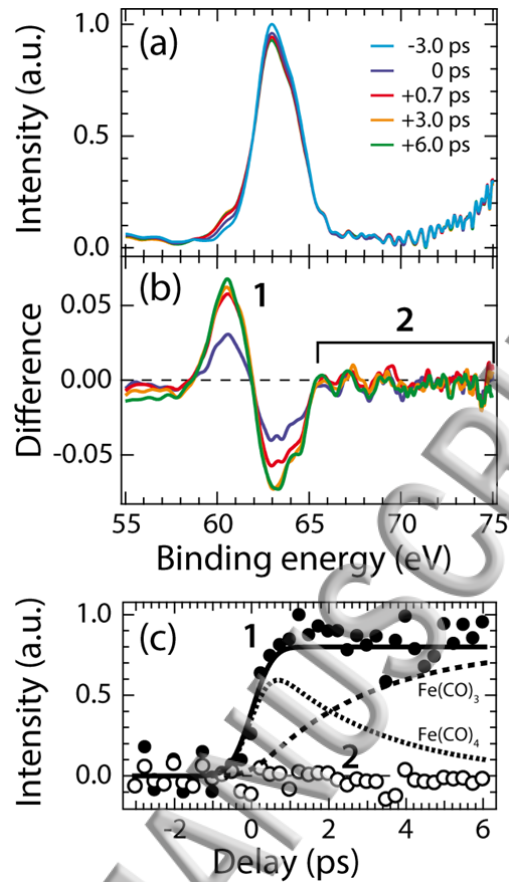


Figure 3. (a) Fe 3p core-level photoelectron spectra of Fe(CO)₅ at indicated delay times after excitation at 266 nm (photon energy 123 eV, intensity of the -3.0 ps spectrum normalized to one at maximum). (b) Difference spectra (the spectrum corresponding to unpumped molecules at -3 ps was subtracted from the intensities at the given delays). (c) Integrated intensities versus pump-probe delay time of the Fe(CO)₄ and Fe(CO)₃ peak (1, closed circles, integration interval 58.5-62 eV, intensities normalized to one at maximum) and of the high-energy side of the Fe 3p peak (2, open circles, integration interval 65.5-75 eV) with the kinetic model (solid lines) taken from Fig. 2 without changes.

More interestingly, we find no intensity arising on the high-binding energy side of the Fe 3p line at 65-75 eV (see region 2 in Fig. 3(b)). Intensity of region 2 is constant at zero within the 6 ps measured here within the statistical uncertainty of our experiment (Fig. 3(c)). This absence of intensity proves that Fe(CO)₄ and Fe(CO)₃ occur in a singlet state as is explained with the help of Fig. 4.

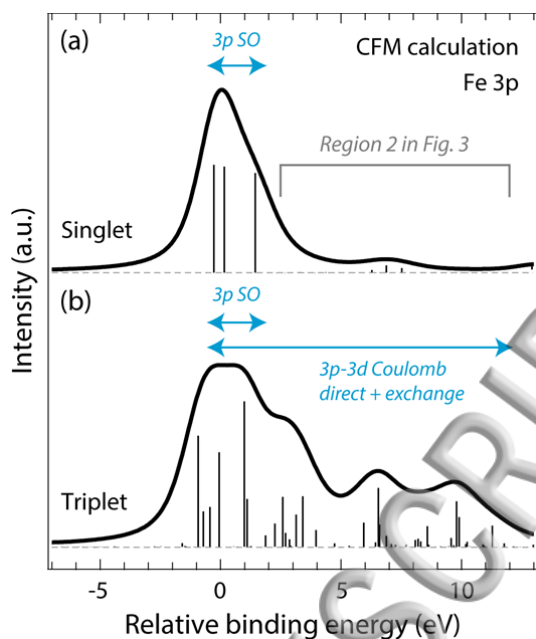


Figure 4. Fe 3p photoelectron spectra calculated within the crystal-field multiplet model (CFM) representing (a) singlet and (b) triplet states of, within the approximations of the CFM model, $\text{Fe}(\text{CO})_5$, $\text{Fe}(\text{CO})_4$ and $\text{Fe}(\text{CO})_3$. Sticks are calculated binding energies and transition intensities of the final ionic $3p^{-1}$ core-hole states. Spectra were aligned to 0 eV at maximum for easier comparison of the shapes with intensities normalized at maximum.

Our approach for determining the spin state is based on using the localized 3p core hole on Fe and the induced local atomic multiplet effects to extract the ground-state multiplicity of $\text{Fe}(\text{CO})_4$ and $\text{Fe}(\text{CO})_3$. Fadley and co-workers established that the 3p photoelectron spectrum of 3d transition-metal atoms and ions in open-shell (high-spin) configurations exhibits atomic multiplet effects due to the strong core-valence 3p-3d Coulomb direct and exchange interactions in the final ionic states thus spreading the spectrum over more than 10 eV to the higher binding-energy side of the main 3p line^{39, 40}. Closed-shell (low-spin) configurations in contrast, such as in the Cu atom, show a single peak⁴¹ merely broadened by 3p spin-orbit interactions of 1-2 eV^{41, 42}. With our crystal-field multiplet model (CFM) calculations for $\text{Fe}(\text{CO})_5$, $\text{Fe}(\text{CO})_4$ and $\text{Fe}(\text{CO})_3$ in Fig. 4 we extend this approach to infer the multiplicity of the transient intermediates $\text{Fe}(\text{CO})_4$ and $\text{Fe}(\text{CO})_3$. For singlet states, the Fe 3p photoelectron spectrum exhibits one peak thus well describing singlet-state $\text{Fe}(\text{CO})_5$. In hypothetical triplet states, the 3p-3d core-valence interactions spread the multiplet to higher binding energies over more than 10 eV. Intensity in this region (region 2 in Fig. 3) is therefore a sensitive measure of the spin-state of $\text{Fe}(\text{CO})_4$ and $\text{Fe}(\text{CO})_3$. The absence of intensity in this region in

Our time-resolved core-level photoelectron spectra thus unambiguously prove that neither the transient intermediate $\text{Fe}(\text{CO})_4$ nor $\text{Fe}(\text{CO})_3$ on time scales up to 6 ps occur in a triplet state. This directly validates the proposed singlet pathway for $\text{Fe}(\text{CO})_5$ photodissociation²¹. It also demonstrates the complementarity of time-resolved 3p photoelectron and K_β fluorescence spectroscopy⁴³ for determining the multiplicity of 3d transition-metal centers in inorganic and organometallic photoreactions^{44, 45} as both owe their sensitivity to the same 3p-3d core-valence interactions.

In summary, the photodissociation of the prototypical organometallic compound $\text{Fe}(\text{CO})_5$ in the gas phase is investigated with optical pump and x-ray probe photoelectron spectroscopy at an x-ray free-electron laser. Our data prove successive dissociation to $\text{Fe}(\text{CO})_4$ in a first step with subsequent dissociation to $\text{Fe}(\text{CO})_3$ in a second step. We unambiguously find that neither the transient intermediate $\text{Fe}(\text{CO})_4$ nor $\text{Fe}(\text{CO})_3$ on time scales up to 6 ps occur in their triplet ground states. This validates the proposed singlet pathway for $\text{Fe}(\text{CO})_5$ photodissociation²¹. Our time-resolved observation of singlet-state $\text{Fe}(\text{CO})_4$ can guide future studies that aim at making use of the high reactivity of this coordinatively unsaturated intermediate. We define a time window of 3 ps during which further dissociation of $\text{Fe}(\text{CO})_4$ as well as dissipative transition to its unreactive triplet state have to be prevented in order to make its excess energy accessible. Our results indicate that solute-solvent interactions possibly involving vibrational relaxation^{12, 13} may be necessary for the formation of triplet-state $\text{Fe}(\text{CO})_4$. With time-resolved core-level photoelectron spectroscopy we selectively probe and follow in time the evolution of the multiplicity of the Fe center thereby benchmarking time-resolved optical pump and x-ray probe photoelectron spectroscopy for extracting spin-density dynamics in organometallic photoreactions. Our results further extend the demonstrated capabilities of time-resolved photoelectron spectroscopy with optical and XUV probe pulses²⁴⁻³¹ thus complementing other time-resolved experimental techniques for the investigation of photochemical reactions⁴⁶⁻⁵⁶.

We cordially thank the FLASH team for excellent support before and during the beamtime and we are grateful in particular to the machine operators, the run coordinators, and Harald Redlin for support in setting up the optical pump laser. This work was supported by the Helmholtz Virtual Institute "Dynamic Pathways in Multidimensional Landscapes" and the Volkswagen Stiftung (M.B.). M.O. acknowledges financial support from the Swedish

Research Council (VR) and the Carl Trygger Foundation. I.J. acknowledges support by the Lennander Foundation. M.M. acknowledges support by the excellence cluster “The Hamburg Center for Ultrafast Imaging – Structure, Dynamics and Control of Matter at the Atomic Scale” of the Deutsche Forschungsgemeinschaft (CUI, DFG-EXC1074). Further support was given by the German Federal Ministry of Education and Research through the priority programme FLASH: “Matter in the light of ultrashort and extremely intense X-ray pulses” and contract number 05K10PK2. P.W. thanks Kelly Gaffney and Albert Schweizer for enlightening discussions.

¹ E. Koerner von Gustorf, and F.-W. Grevels, *Tp. Curr. Chem.* **13** (1969) 366-450.

² M. Wrighton, *Chem. Rev.* **74** (1974) 401-430.

³ N. Leadbeater, *Coord. Chem. Rev.* **188** (1999) 35-70.

⁴ P. Rudolf *et al.*, *J Phys Chem Lett* **4** (2013) 596-602.

⁵ H. Cho *et al.*, *Inorg Chem* **55** (2016) 5895-5903.

⁶ L. Banares *et al.*, *J. Chem. Phys.* **108** (1998) 5799-5811.

⁷ P. T. Snee *et al.*, *J. Am. Chem. Soc.* **123** (2001) 6909-6915.

⁸ P. Wernet *et al.*, *Nature (London)* **520** (2015) 78-81.

⁹ K. Kunnus *et al.*, *Struct. Dyn.* **3** (2016) 043204.

¹⁰ B. Ahr *et al.*, *Phys Chem Chem Phys* **13** (2011) 5590-5599.

¹¹ S. J. Harris *et al.*, *Phys. Chem. Chem. Phys.* **15** (2013) 6567-6582.

¹² T. P. Dougherty, and E. J. Heilweil, *Chem. Phys. Lett.* **227** (1994) 19-25.

¹³ J. T. King, M. R. Ross, and K. J. Kubarych, *J Phys Chem B* **116** (2012) 3754-3759.

¹⁴ M. Poliakoff, and J. J. Turner, *Angew. Chem. Int. Ed.* **40** (2001) 2809-2812.

¹⁵ A. J. Ouderkerk *et al.*, *J. Am. Chem. Soc.* **105** (1983) 3345-3355.

¹⁶ M. Poliakoff, and E. Weitz, *Acc. Chem. Res.* **20** (1987) 408-414.

¹⁷ M. Poliakoff, and J. J. Turner, *J. Chem. Soc., Dalton Transactions* (1974) 2276.

¹⁸ L. A. Barnes, M. Rosi, and C. W. J. Bauschlicher, *J. Chem. Phys.* **94** (1991) 2031-2039.

- ¹⁹ C. Daniel *et al.*, J. Phys. Chem. C **88** (1984) 4805-4811.
- ²⁰ J. N. Harvey, and M. Aschi, Faraday Discussions **124** (2003) 129.
- ²¹ A. A. Trushin *et al.*, J. Phys. Chem. A **104** (2000) 1997-2006.
- ²² H. Ihee, J. Cao, and A. H. Zewail, Angew. Chem. Int. Ed. **40** (2001) 1532-1536.
- ²³ W. Ackermann *et al.*, Nat. Phot. **1** (2007) 336-342.
- ²⁴ A. E. Bragg, A. Stolow, and M. Neumark, Chem. Rev. **104** (2004) 1719-1757.
- ²⁵ H. Dachraoui *et al.*, Phys. Rev. Lett. **106** (2011) 107401.
- ²⁶ O. Geßner *et al.*, Science **311** (2006) 219-222.
- ²⁷ T. Horio *et al.*, J Chem Phys **145** (2016) 044306.
- ²⁸ R. Iikubo *et al.*, J Phys Chem Lett **6** (2015) 2463-2468.
- ²⁹ L. Nugent-Glandorf *et al.*, Phys Rev Lett **87** (2001) 193002.
- ³⁰ P. Wernet, Phys. Chem. Chem. Phys. **13** (2011) 16941-16954.
- ³¹ P. Wernet *et al.*, Phys. Rev. Lett. **103** (2009) 013001.
- ³² G. Grell *et al.*, J. Chem. Phys. **143** (2015) 074104.
- ³³ F. Aquilante *et al.*, J. Comput. Chem. **37** (2016) 506-541.
- ³⁴ F. M. De Groot, and A. Kotani, *Core Level Spectroscopy of Solids* (CRC Press: Boca Raton, FL, 2008),
- ³⁵ F. M. F. De Groot *et al.*, Phys. Rev. B **42** (1990) 5459-5468.
- ³⁶ M. Ohno, and G. A. van Riessen, J. of Electron Spectroscopy and Relat. Phenom. **128** (2003) 1-31.
- ³⁷ R. Fukuda *et al.*, J. Chem. Phys. **132** (2010) 084302.
- ³⁸ E. Sistrunk *et al.*, J. Chem. Phys. **139** (2013) 164318.
- ³⁹ C. S. Fadley *et al.*, Phys. Rev. Lett. **23** (1969) 1397-1401.
- ⁴⁰ B. Hermsmeier *et al.*, Phys. Rev. Lett. **61** (1988) 2592-2595.

- ⁴¹ M. Martins *et al.*, J. Phys. B **39** (2006) R79-R125.
- ⁴² A. von dem Borne *et al.*, Phys. Rev. A **62** (2000)
- ⁴³ P. Glatzel, and U. Bergmann, Coord. Chem. Rev. **249** (2005) 65-95.
- ⁴⁴ G. Vanko *et al.*, J. Phys. Chem. C **119** (2015) 5888-5902.
- ⁴⁵ W. Zhang *et al.*, Nature (London) **509** (2014) 345-348.
- ⁴⁶ M. Dell'Angela *et al.*, Science **339** (2013) 1302-1305.
- ⁴⁷ M. Eckstein *et al.*, Phys. Rev. Lett. **116** (2016) 163003.
- ⁴⁸ T. W. Kim *et al.*, Phys. Chem. Chem. Phys. **18** (2016) 8911-8919.
- ⁴⁹ P. M. Kraus, and H. J. Wörner, Chem. Phys. **414** (2013) 32-44.
- ⁵⁰ W. Li *et al.*, Science **322** (2008) 1207-1211.
- ⁵¹ M. P. Minitti *et al.*, Phys. Rev. Lett. **114** (2015) 255501.
- ⁵² Y. Ogi *et al.*, Struct. Dyn. **2** (2015) 034901.
- ⁵³ J. Vura-Weis *et al.*, J. Phys. Chem. Lett. **4** (2013) 3667-3671.
- ⁵⁴ N. A. Miller *et al.*, J Am Chem Soc **139** (2017) 1894-1899.
- ⁵⁵ B. E. Van Kuiken *et al.*, J Phys Chem Lett **3** (2012) 1695-1700.
- ⁵⁶ L. Drescher *et al.*, J Chem Phys **145** (2016) 011101.

